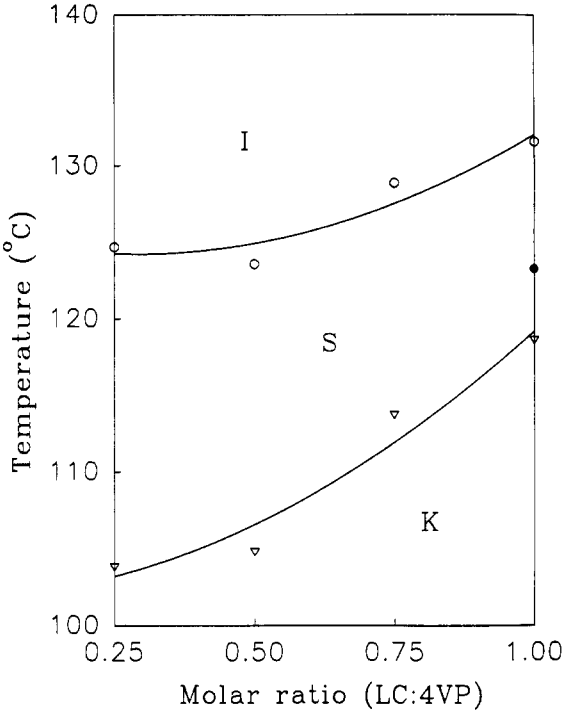


**Figure 4.** Maxima of the DSC transitions in the cooling thermograms (5 °C/min) of the mixtures of functionalized liquid crystal with poly(4-vinylpyridine) as a function of molar ratio. I, S, and K represent the isotropic, disordered smectic, and crystalline phases, respectively.

both heating and cooling. The temperatures of their maxima are somewhat lower than those for the pure LC. Furthermore, the transition to and from the isotropic liquid is the predominant transition, and it is very sharp compared to that for the pure LC. X-ray scattering results (Figure 2b) show that the phase between the two transitions has the same structure as the disordered phase of the pure LC; only the small-angle Bragg spacing, at 19.3 Å, is somewhat smaller for the mixture than it is for the LC by itself. It is also evident from the X-ray measurements that the phase which exists on cooling in the pure LC, and which has disappeared in the mixture, is the higher temperature ordered phase.

When the molar ratio of the mixture is varied, DSC results (Figure 4) demonstrate that the disordered phase is extended over a significantly wider temperature region with decrease in the molar ratio of LC to 4VP (P4VP repeat unit) from 1:1 to 0.25:1. This is in contrast to our preliminary results of mixtures of the same LC with poly(acrylic acid). In the latter case, the thermal stability of the disordered phase *decreases* considerably, to less than 2 °C between the maxima of the two transitions at a molar ratio of 0.25:1. In these mixtures, hydrogen-bonded acid pairs involving the functionalized LC and the polymer are not expected to be favored as in the LC/P4VP mixture. It is also to be noted that, for the mixtures with P4VP, the intermediate phase in the pure LC is absent in all mixtures of molar ratios less than 1:1. Distinct glass transition temperatures were not detected by DSC; this phenomenon has been noted previously in side-chain LC polymers.[11]

In conclusion, the results described above indicate that the H-bonding interactions between the acid group of the functionalized LC and the pyridine group of the polymer are sufficient to thermally stabilize the disordered phase which is existent in the LC alone. The stabilization increases as the molar ratio of LC to 4VP is diminished, in the range studied. We are currently completing our studies of the LC/P4VP mixtures at various molar ratios, as well as investigating their dynamic mechanical properties.

**Acknowledgment.** We thank NSERC (Canada) and FCAR (Québec) for financial support.

(11) Mallon, J. J.; Kantor, S. W. *Macromolecules* **1990**, *23*, 1249.

## Second Order Optical Nonlinearity on a Modified Sol-Gel System at 100 °C

R. J. Jeng, Y. M. Chen, A. K. Jain, J. Kumar, and S. K. Tripathy*

*Departments of Chemistry and Physics*
*University of Massachusetts/Lowell*
*Lowell, Massachusetts 01854*

*Received June 5, 1992*
*Revised Manuscript Received July 21, 1992*

Second-order nonlinear optical (NLO) properties of polymeric materials have been widely studied.[1] Polymeric materials have become competitive with inorganics for nonlinear optical applications such as fast waveguide electrooptic modulation and frequency-doubling devices provided the nonlinearity shows reasonable stability at ambient temperatures. The noncentrosymmetric alignment of the NLO chromophores that results from the poling process is not in a state of thermodynamic equilibrium. Therefore, the alignment would relax to a random configuration in the absence of a poling field. To prevent the randomization of the poled molecules, the NLO chromophores are usually incorporated in a polymer which has a high glass transition temperature ($T_g$). This is due to the fact that the molecular orientational motion is closely associated with the $T_g$ of the polymer. Moreover, enhanced temporal stability of second-order NLO properties in a poled polymer system can be obtained when a certain degree of cross-linking is introduced. In the cross-linked polymer, the NLO moieties are either incorporated or covalently bound into a rigid polymer network and are much less likely to relax to random orientation. The polymers can be cross-linked by thermal means[1e,f,2] or by photochemical means.[3]

Sol-gel technology provides an attractive route to the preparation of a three-dimensional inorganic network.[4] The basic sol-gel process involves the sequential hydrolysis

(1) (a) Daigo, H.; Okamoto, N.; Fujimura, H. *Opt. Commun.* **1988**, *69*, 177. (b) Mortazavi, M.; Knoesen, A.; Kowel, S.; Higgins, B.; Dienes, A. *J. Opt. Soc. Am.* **1989**, *B6*, 733. (c) Hampsch, H.; Yang, J.; Wong, G.; Torkelson, *J. Macromolecules* **1990**, *23*, 3640. (d) Hayden, L.; Sauter, G.; Ore, F.; Pasillas, P.; Hoover, J.; Lindsay, G.; Henry, R. *J. Appl. Phys.* **1990**, *68*, 456. (e) Hubbard, M.; Marks, T.; Yang, J.; Wong, G. *Chem. Mater.* **1989**, *1*, 167. (f) Reck, B.; Eich, M.; Jungbauer, D.; Twieg, R.; Willson, C.; Yoon, D.; Bjorklund, G. *SPIE, Proc.* **1989**, *1147*, 74. (g) Jungbauer, D.; Teraoka, I.; Yoon, D.; Reck, B.; Swalen, J.; Twieg, R.; Willson, C. *J. Appl. Phys.* **1991**, *69*, 8011.

(2) (a) Eich, M.; Reck, B.; Yoon, D.; Willson, C.; Bjorklund, G. *J. Appl. Phys.* **1989**, *66*, 3241. (b) Jungbauer, D.; Reck, B.; Twieg, R.; Yoon, D.; Willson, G.; Swalen, J. *Appl. Phys. Lett.* **1990**, *56*, 2610. (c) *Jeng*, R.; Chen, Y.; Kumar, J.; Tripathy, S. *J. Macromol. Sci.—Pure Appl. Chem.*, in press. (d) Jeng, R.; Chen, Y.; Tripathy, S.; Kumar, J. *Opt. Commun.* **1992**, *89*, 212.

(3) (a) Mandal, B.; Chen, Y.; Lee, J.; Kumar, J.; Tripathy, S. *Appl. Phys. Lett.* **1991**, *58*, 2459. (b) Chen, M.; Yu, L.; Dalton, L.; Shi, Y.; Steier, W. *Macromolecules* **1991**, *24*, 5421. (c) Mandal, B.; Kumar, J.; Huang, J.; Tripathy, S. *Makromol. Chem. Rapid Commun.* **1991**, *12*, 63. (d) Tripathy, S.; Mandal, B.; Jeng, R.; Lee, J.; Kumar, J. *Polym. Prepr. (Am. Chem. Soc., Div. Polym. Chem.)* **1991**, *32*, 4.

(4) (a) *Sol-Gel Science*; Brinker, C., Scherrer, G., Eds.; Academic Press: Orlando, FL. 1990. (b) Wynne, K.; Rice, R. *Annu. Rev. Mater. Sci.* **1984**, *14*, 297.

0897-4756/92/2804-0972$03.00/0 

**Chart I. Inorganic Network**

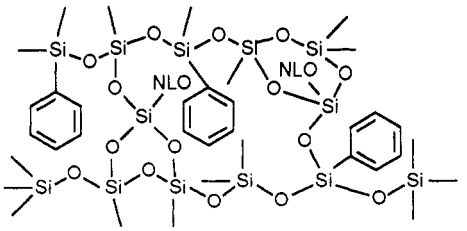


**Scheme I. Reaction Mechanism of the Sol–Gel Process**

hydrolysis

$$\equiv SiOR + HOH \rightleftarrows \equiv SiOH + ROH$$

water condensation

$$\equiv SiOH + HOSi\equiv \rightleftarrows \equiv SiOSi\equiv + HOH$$

alcohol condensation

$$\equiv SiOH + ROSi\equiv \rightleftarrows \equiv SiOSi\equiv + ROH$$

and polycondensation of silicon alkoxide at temperatures that are commonly used to process polymeric materials[5] (Scheme I).

Curing at higher temperatures leads to further cross-linking of the inorganic matrix but may also result in degradation of the NLO chromophores. It is known that at low temperature the condensation requires many hours or days; higher temperatures (>150 °C) shorten the curing time.[5a] Numerous chromophores have been incorporated into glassy materials, for instance, laser dye or $\pi$-conjugated NLO polymer.[6] Recently, a cross-linked guest–host system with an NLO dye, disperse red 1, in a cross-linked phenylsiloxane polymer matrix was reported by us.[2d] This cross-linked guest–host system has excellent temporal stability at room temperature and shows a slow decay in $d_{33}$ at 100 °C in a period of 30 h. Recently there have been other reports on NLO sol–gel process, where large concentrations of NLO chromophores have been chemically bonded to the silicon oxide backbone of the inorganic network by attaching the NLO chromophore directly to the silicon atom.[5b,7] However, these materials have not been characterized for the stability of second-order optical nonlinearity at both room temperature and elevated temperatures.

In this communication we report our investigations on a cross-linked guest–host system based on a newly synthesized alkoxysilane dye and phenylsiloxane polymer used earlier.[2d] Upon heating to high temperatures, the phenylsiloxane polymer containing hydroxyl and ethoxyl groups, and alkoxysilane dye lead to a cross-linked network (Chart I). Phenylsiloxane polymers have been processed at high temperatures (to 460 °C) to lead to optically clear low loss glasses. The guest–host samples can be poled and cured simultaneously. This ensures that the NLO dye will be locked in the three-dimensional network of the glass matrix in a noncentrosymmetric manner with acceptably slow relaxation even at elevated temperatures. We report on the stability at room temperature and at 100 °C of the second-order nonlinearity of the cured polymer films. The

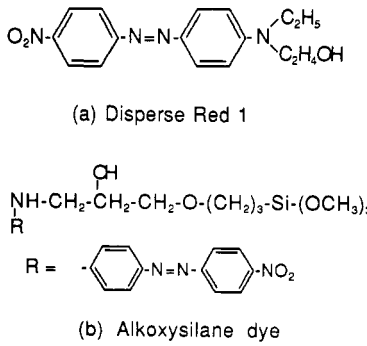


**Figure 1.** Chemical structures of disperse red 1 and alkoxysilane dye.

linear and second-order nonlinear optical properties of poled and cured phenylsiloxane polymer/alkoxysilane dye were measured at 1.06 $\mu$m and are reported. For the sake of comparison, the behavior of the cured phenylsiloxane polymer/DR1 is also discussed.

The samples for which data are presented use Accuglass 204 (A204), a phenylsiloxane polymer dissolved in alcohol and available from Allied Signal. The formula for the compound provided by the manufacturer is as follows:

$$[(SiO)_a(C_6H_5)_b(OC_2H_5)_c(OH)_d]_n$$

$$a \geq 1; \quad b, c, d \leq 0.5; \quad n = 5\text{–}100$$

The guest molecule disperse red 1 (DR1), 4-[ethyl(2-hydroxyethyl)amino]-4′-nitroazobenzene (Figure 1) is available from Aldrich Chemical and was recrystallized from benzene. DR1 (35 mg) in 0.15 g of 1,4-dioxane was added to 2 g of A204 solution. In addition, the alkoxysilane dye (ASD, Figure 1) was synthesized by the coupling of a monoepoxy of (3-glycidoxypropyl)trimethoxysilane and a monoamine of 4-(4′-nitrophenylazo)phenylamine (so called disperse orange 3).[8] ASD (0.10 g) in 0.50 g of acetone was added into 4 g of A204 solution. Films were prepared by spin-coating the dye/siloxane polymer solutions onto 1-mm-thick transparent microscope slides (Fisher Premium) and then baked at 70 °C under vacuum for 12 h to remove residual solvent trapped in samples. Typical thickness obtained were approximately 760 and 690 nm for the cured A204/DR1 and A204/ASD, respectively. Indices of refraction at two different wavelengths (532 and 1064 nm) were measured using an ellipsometer. The absorption characteristics of the NLO molecules in the polymeric film were recorded on a UV–vis–near-IR spectrophotometer.

The film was poled by the corona discharge method. The details of the corona poling setup have been reported earlier.[9] After the sample was poled at 80 °C for 6 min, the temperature was increased to 200 °C to vitrify the sample. During this period (curing time) the poling field was kept on. The sample was maintained at 200 °C for 10 min and then cooled down to room temperature with the poling field on. The curing temperature was chosen to be 200 °C because the thermal decomposition temperatures of ASD and DR1 were determined to be approximately 237 and 254 °C, respectively, by a thermogravimetric analyzer (Du Pont TGA2950) at a heating rate of 10 °C/min in air.

The second-order NLO properties of the poled A204/DR1 and A204/ASD samples was measured by second

(5) (a) Hardman, B.; Torkelson, A. In *Encyclopedia of Polymer Science and Engineering*; Wiley: New York, 1986; Vol. 15, p 252. (b) Kim, J.; Plawsky, J.; LaPeruta, R.; Korenowski, G. *Chem. Mater.* **1992**, *4*, 249. (c) Coltrain, B.; Ferrar, W.; Landry, C.; Molaire, T.; Zumbulyadis, N. *Chem. Mater.* **1992**, *4*, 358.

(6) (a) Haruvy, Y.; Webber, S. *Chem. Mater.* **1991**, *3*, 501. (b) Wung, C.; Pang, Y.; Prasad, P.; Karasz, F. *Polymer* **1991**, *32*, 605.

(7) Puccetti, G.; Toussaere, E.; Ledoux, I.; Zyss, J.; Griesmar, P.; Sanchez, C. *Polym. Prepr. (Am. Chem. Soc., Div. Polym. Chem.)* **1991**, *32*, 61.

(8) (a) Mandal, B.; Jeng, R.; Kumar, J.; Tripathy, S. *Makromol. Chem. Rapid Commun.* **1991**, *12*, 607. (b) Lee, H.; Nevelle, K. *Handbook of Epoxy Resins*; McGraw-Hill: New York, 1967.

(9) Mandal, B.; Chen, Y.; Jeng, R.; Takahashi, T.; Huang, J.; Kumar, J.; Tripathy, S. *Eur. Polym. J.* **1991**, *27*, 735.

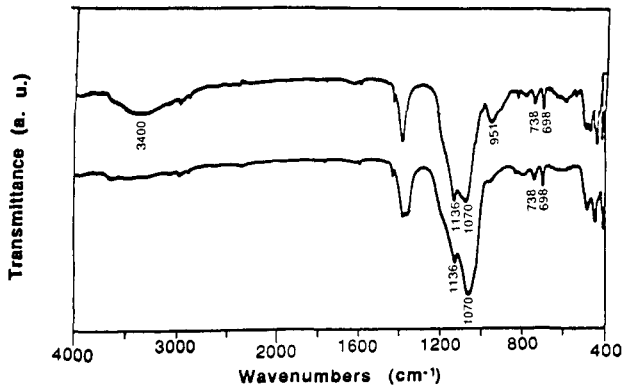


**Figure 2.** Infrared spectra of Accuglass 204, from top to bottom: pristine, cured.

**Table I. Optical Properties of the Cured A204/DR1 and A204/ASD**

| | A204/DR1 | A204/ASD |
|---|---|---|
| thickness (μm) | 0.76 | 0.69 |
| refractive indexes λ (μm) | | |
| 0.532 | 1.628 | 1.537 |
| 1.000 | 1.527 | 1.504 |
| $d_{33}$ (pm/V) at 1.06 μm | 11.43 | 5.28 |

harmonic generation (SHG). The polarized Q-switched Nd:YAG laser with 10-ns pulse width and 20-Hz repetition rate was used as the light source. The typical energy per pulse of the laser was 15 mJ. The fundamental laser beam after passing through the sample was blocked by $CuSO_4$ solution and a 532-nm interference filter. The second harmonic signal was detected by a photomultiplier tube, and averaged over 300 pulses in a boxcar integrator. The SH intensity of a Y-cut single crystal of quartz with known thickness and $d_{11}$ value ($d_{11}$ = 0.364 pm/V)[10] was measured as a reference mounted at the same position as that of the sample. The detailed experimental setup and calculations of the second-order NLO coefficient $d_{33}$ have been previously discussed.[11] In addition, the $d_{33}$ values were corrected for absorption.[3a]

After curing of A204 at 200 °C for 10 min an appreciable decrease of absorbance in IR spectra is observed due to the disappearance of hydroxyl groups around 3400 $cm^{-1}$, Si–ethoxyl bonds at 1136 $cm^{-1}$, and hydroxyl and ethoxyl groups at 951 $cm^{-1}$ (Figure 2).[12] Monosubstituted phenyl ring attachment to Si can be identified by the absorption peaks at 738 and 698 $cm^{-1}$. The absorbances of these two peaks decrease slightly after curing. The absorption peak of Si–O–Si (1070 $cm^{-1}$) increases moderately after curing.[12] From the IR spectrum, enhanced formation of the Si–O–Si linkage due to thermal condensation with the removal of the hydroxyl and ethoxyl moieties is clearly indicated. It is important to note that the IR data also indicates that the NLO chromophores were not degraded during the curing process. The cured A204/DR1 and A204/ASD samples were soaked in THF (a good solvent for both DR1 and ASD) for 2 h. The solvent did not extract any measurable concentration of dye from the cured sample. This implies that the NLO dye is firmly locked in the glass matrix.

The second-order NLO properties of A204/DR1 and A204/ASD have been characterized by second harmonic

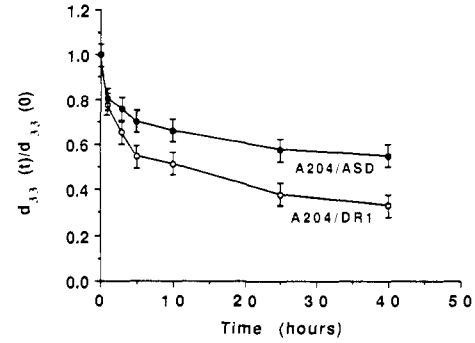


**Figure 3.** Time behavior of the second harmonic coefficient of A204/DR1 and A204/ASD at 100 °C.

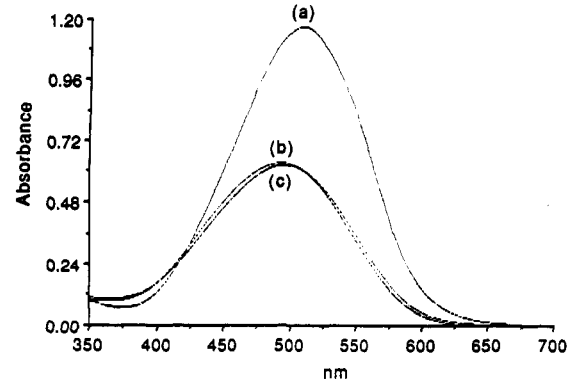


**Figure 4.** UV–vis absorption spectra of A204/DR1, from top to bottom: (a) pristine; (b) right after poling/curing; (c) poled/cured samples, thermal treatment at 100 °C for 40 h.

generation. The $d_{33}$ values obtained for the 1064-nm fundamental wavelength are listed in Table I along with some linear optical properties. The poled and cured films have $d_{33}$ values of 11.43 and 5.28 pm/V for A204/DR1 and A204/ASD, respectively. Despite the fact that A204/DR1 and A204/ASD have similar dye chromophore density in the polymer matrix, the poled/cured A204/DR1 has a larger $d_{33}$ value. This is due to the fact that DR1 has a larger nonlinear hyperpolarizability ($\mu\beta$) compared with disperse orange[13] 3, and a higher order parameter is obtained in the poling process under the same poling condition.

The temporal stability at 100 °C of second order nonlinearity after poling and cross-linking of A204/DR1 and A204/ASD has been investigated (Figure 3). The results clearly indicate that the poled and cured guest–host system, A204/ASD, has much better stability. After over 40 h at 100 °C, a reduction of 45% in $d_{33}$ was observed for the poled and cured A204/ASD. Most of this loss was in the first few hours of heating. On the other hand, a reduction of 67% in $d_{33}$ was observed for the poled/cured A204/DR1 after the same thermal treatment. There are two factors responsible for this. As mentioned earlier, the ASD can be chemically bonded into the cured phenylsiloxane polymer matrix. The bonding between ASD and the cured siloxane polymer restricts the molecular motion of the segments and hence prevents the randomization of the ordered NLO molecules. Second, the size of ASD is much larger than DR1. On the basis of free volume theory, the molecule with smaller size tends to randomize faster in the polymer matrix.

In addition, the nonlinear optical coefficients ($d_{33}$) of the poled/cured A204/DR1 and A204/ASD remained un-

(10) *Handbook of Optical Constants*; Palik, E., Ed.; Academic Press: Orlando, 1985.

(11) (a) Jerphagnon, J.; Kurtz, S. *J. Appl. Phys.* **1970**, *41*, 1667. (b) Singer, K.; Sohn, J.; Lalama, S. *Appl. Phys. Lett.* **1986**, *49*, 248.

(12) (a) *Analysis of Silicons*; Smith, A., Ed.; Wiley-Interscience: New York, 1974. (b) *The Infrared Spectra of Complex Molecules*, 3rd ed.; Bellamy, L., ed.; Chapman and Hall: London, 1975.

(13) Singer, K.; Sohn, J.; King, L.; Katz, H.; Dirk, W. *J. Opt. Soc. Am.* **1989**, *B6*, 1339.

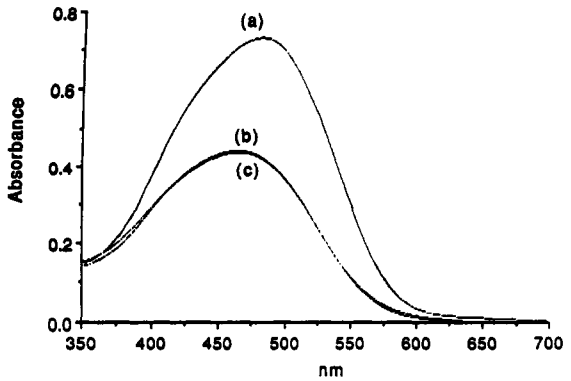


**Figure 5.** UV-vis absorption spectra of A204/ASD, from top to bottom: (a) pristine; (b) right after poling/curing; (c) poled/cured samples, thermal treatment at 100 °C for 40 h.

changed under ambient condition for at least 40 h, time to which these measurements were carried out.

To investigate the absorption behavior as a function of time, the absorption spectrum at 100 °C was taken at regular intervals over 40 h for poled/cured A204/DR1. An absorption peak at $\lambda_{max}$ = 508 nm existed before poling/curing. After poling/curing $\lambda_{max}$ shifts to 493 nm with a decrease of absorbance. During the next 40 h, $\lambda_{max}$ shifted back toward longer wavelengths with a slight decrease in absorbance (Figure 4). It is important to note that the dye absorption spectrum shape is similar to the spectrum obtained before the curing cycle. This confirms that the azo dye left in the cured film has not degraded during the curing cycle.

For A204/ASD, the absorption spectrum was also taken regularly at 100 °C over 40 h. Immediately after poling/curing, a decrease in absorbance was observed. The absorption peak of the disperse orange 3 chromophore ($\lambda_{max}$ = 480 nm) shifted toward shorter wavelength, $\lambda_{max}$ = 464 nm (Figure 5). During the next 40 h, the absorption spectrum remained unchanged. This result suggests that the dye/polymer system did not degrade or sublime throughout the whole period of thermal treatment.

In conclusion, we have shown that a guest-host system based on cross-linked phenylsiloxane polymer and alkoxysilane dye has excellent room-temperature stability and a slow decay at 100 °C in a period of 40 h. The stability of second-order susceptibility achieved in this work is limited by the NLO chromophore degradation temperature. Curing at higher temperatures is clearly expected to lead to higher stability. However the A204/ASD thin film showed a much more stable second-order response compared to A204/DR1.

**Acknowledgment.** Partial financial support from ONR is gratefully acknowledged.

## Molecular Sieve Sensors for Selective Ethanol Detection

Yongan Yan and Thomas Bein*

*Department of Chemistry, Purdue University*
*West Lafayette, Indiana 47907*

*Received March 9, 1992*
*Revised Manuscript Received June 16, 1992*

Chemical microsensors play an increasing role in the area of environmental monitoring and industrial processing.[1]

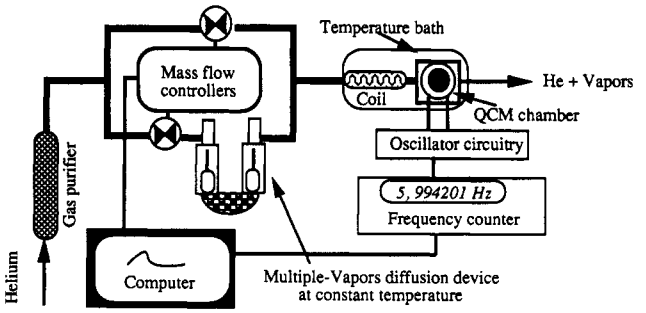


**Figure 1.** Schematic diagram of the apparatus for multiple vapor sorption experiments with the microsensor.

We have recently developed microsensors with molecular sieving functions in chemically selective layers on piezoelectric devices.[2-4] Here we report the development of a chemical microsensor with *combined* molecular sieve and selective surface interactions, based on novel silicalite-silica composite thin films on the active areas of quartz crystal microbalances (QCMs).

In addition to the high sensitivity and selective size exclusion offered by molecular sieve micropore films, the nature of the chemical surface interactions is important. In the thin films described below, interference from water (2.65 Å) which is smaller than ethanol (4.3 Å), could be minimized through hydrophobicity of the molecular sieve and the matrix (silica). The interplay of size exclusion and surface affinity thus provides highly selective adsorption suitable for sensor applications.

The QCM used in the present study is an AT-cut 6-MHz piezoelectric resonator, with 0.20 $cm^2$ gold electrodes deposited on chromium underlayers on opposite sides of the crystal. The sensitivity of the QCM according to the Sauerbrey relationship[5] is 12.3 ng $Hz^{-1}$ $cm^{-2}$. The electrode surface area resulting from the surface roughness evaluated by nitrogen sorption isotherms at -196 °C is 2.60 $cm^2/cm^2$.

The preparation of the microporous layer involved two steps: First, silicalite crystals (about 3-$\mu$m diameter) were chemically anchored to the QCM gold electrodes via a thiol-organosilane coupling layer.[4] Silicalite is a crystalline molecular sieve of approximate composition $SiO_2$ with a pore system of zigzag channels along *A* (free cross section ca. 5.1 × 5.5 Å), linked by straight channels along *B* (5.3 × 5.6 Å).[6] The silicalite crystals bonded to the QCM electrodes were then further coated with an amorphous, porous silica layer, prepared via sol-gel processing from $Si(OEt)_4$,[7] so that stable microporous thin films composites were obtained.[8] Typical film compositions are 0.50 $\mu g/cm^2$

* To whom correspondence should be addressed.

(1) For recent reviews see: (a) Janata, J. *Anal. Chem.* **1990**, *62*, 33r. (b) Hughes, R. C.; Ricco, A. J.; Butler, M. A.; Martin, S. J. *Science* **1991**, *254*, 75.

(2) (a) Bein, T.; Brown, K.; Frye, G. C.; Brinker, C. J. U.S. Patent Application 07/580,373, allowed on Jan 23, 1992, to be issued. (b) Bein, T.; Brown, K.; Frye, G. C.; Brinker, C. J. *J. Am. Chem. Soc.* **1989**, *111*, 7640.

(3) Bein, T.; Brown, K.; Brinker, C. J. *Stud. Surf. Sci. Catal.* **1989**, *49*, 887.

(4) Yan, Y.; Bein, T. *J. Phys. Chem.*, in press.

(5) $\Delta f = -2f_0^2 \Delta m A^{-1}(\rho_q \mu_q)^{-1/2}$, where $\Delta f$ is frequency shift, $f_0$ the parent frequency of the QCM, $\Delta m$ the mass change in grams, *A* the piezoelectrically active area in $cm^2$, $\rho_q$ the density (2.648 g $cm^{-3}$), and $\mu_q$ the shear modulus ($2.947 \times 10^{11}$ dyn $cm^{-2}$) for AT-cut quartz. See: Sauerbrey, G. *Z. Phys.* **1959**, *155*, 206.

(6) (a) Flanigen, E. M.; Bennett, J. M.; Grose, R. W.; Cihen, J. P.; Patton, R. L.; Kirchner, R. M.; Smith, J. V. *Nature* **1978**, *271*, 512. (b) Meier, W. M.; Olson, D. H. *Atlas of Zeolite Structure Types*, 2nd ed.; Butterworth: London, 1987.

(7) Bein, T.; Yan, Y. U.S. Patent, in preparation.

0897-4756/92/2804-0975$03.00/0 